MENOUFIA JOURNAL OF AGRICULTURAL BIOTECHNOLOGY

https://mjab.journals.ekb.eg

EFFECT OF ZINC OXIDE NANOPARTICLES ON ANTIBIOTIC RESISTANCE OF *STAPHYLOCOCCUS AUREUS* ASSOCIATED WITH DIABETIC FOOT ULCERS

Hussein, A.[(1)]; Elbeltagy, A.[(2)]; Mansour, S.[(3)] and Fahim, S.[(2)*]

[(1)] Saudi German Hospital, Laboratory and blood bank Dept., Cairo, Egypt.

[(2)] Agri. Microbiology, Botany Dept., Fac. Agri., Menoufia Univ., Egypt.

[(3)] Agri. Biochemistry Dept., Fac. Agri, Menoufia University, Egypt.

Received: Mar, 16, 2025 Accepted: Apr. 5, 2025

ABSTRACT: Over the past decade, the rising prevalence of antibiotic resistance has posed a significant challenge to the effective treatment of numerous bacterial infections. Creating novel antimicrobial biomaterials, which unavoidably have expanded therapeutic possibilities in medical methods, also requires innovative nanomaterials. It prompts several attempts to develop novel metal oxide nanoparticles (NPs) to more effectively control the Multi Drug Resistant (MDR) bacteria responsible for diabetic foot ulcers. This work used the sol-gel method to produce zinc oxide nanoparticles, which were then characterized by X-ray diffraction, Fourier-transformed infrared, and transmission electron microscopy. The pure phase of non-agglomerated ZnO-NPs with diameters ranging from 30 to 50 nm and an average diameter of 40 nm was synthesized using the employed approach in conjunction with TEM analysis. The TEM examination indicates that the morphology of ZnO-NPs has developed to be nearly hexagonal. On the other hand, the infection by MDR S. aureus represented 21.3 % of the causes of staphylococcal diabetic foot ulcers. The treatment by ZnO-NPs inhibited the growth of Methicillin, heterogenous Oxacillin Resistant or Vancomycin Intermediated *S. aureus* (MRSA, ORSA, and VISA) phenotypes with an average MIC of 5.21 mM/ml. At the same time, they give MIC average values of 3.49, 2.6, 2.99, and 1.99 µg/ml for (OX, FOX, VA, and LN) individual antibiotics, respectively. In the same aspect, using syn-MICs of antibiotics and ZnO-NPs by (1:1) decreased values by a synergistic effect percentage of 309, 441, 299, and 316 %, respectively. This finding indicates a synergistic effect of combining ZnO-NPs and the tested antibiotics. This result suggests a synergistic interaction between ZnO-NPs and the tested antibiotics. According to the findings, ZnO-NPs are promising nano metal oxides that are useful for diabetic foot ulcer nanomedical therapy strategies.

Keywords: ZnO-nanoparticles; antibiotic-resistant bacteria; diabetic foot ulcers.

INTRODUCTION

Scientific interest in developing new antimicrobial drugs with broad-spectrum activity to supplement or perhaps replace traditional antibiotics has increased due to rising antibiotic resistance (AR) **(**Wang *et al*., 2017). The synergistic effect of antibiotic combinations exceeds the sum of the individual effects of each. This synergistic action was studied to reveal the invitro antimicrobial efficacy of lipopeptides against laboratory models of multidrug-resistant Escherichia coli, Fahim and Hussein (2017). There are two main categories of antimicrobial agents, organic and inorganic. Over the past decade, since inorganic materials like metal and metal oxides are safe and effective at withstanding severe environments, they have garnered more interest (Jacob *et al*., 2014). Some synthetic metal oxide nanoparticles (NPs), including copper, zinc, and ferric oxide, exhibit strong antibacterial properties. The special qualities of inorganic zinc oxide nanoparticles (ZnO-NPs), including their antibacterial, wound-healing, low toxicity, biocompatibility, and good chemical stability, make them particularly interesting (Zhao *et al*., 2014). Since zinc is an essential trace element for the synthesis, stabilization, and operation of proteins and enzymes, ZnO-NPs can also be used as safe

* Corresponding author: sameh_fahim@hotmail.com

antibacterial agents for dermatological applications, making them potentially bi-functional materials (Seker *et al*., 2014). Furthermore, most elements that constitute metal oxides are recognized as trace elements essential to human health (Pati *et al*., 2014). As a result, adding antimicrobial metal oxide nanoparticles (NPs) to skin and dental biomaterials is highly desired (Verma *et al*., 2014). Wet chemical synthesis of metal oxide nanoparticles is a fascinating branch of nanotechnology due to the simplicity and affordability of wet chemical procedures. The shape, surface area, and particle size of metal oxides have all been found to be closely related to their antibacterial activity. For instance, because of their capacity to interact with and harm microbial membranes, metal oxide particles with larger surface areas and a smaller size, no more than 100 nm, have demonstrated enhanced antibacterial action (Jordon *et al*., 2011). More attention should be paid to nosocomial infections than is currently occurring. The morbidity and mortality rates among hospitalized patients make it a serious issue. The problem is difficult to control because of the lack of a consistent methodology and the unavailability of records, statistics, and information (Rahman *et al*., 2011). Microbial infections represent between 50 and 75% of hospitalized patients' morbidity. One of the most dangerous side effects that arise in the earliest stages of diabetes treatment is diabetic ulcer (Saxena *et al*., 2013). Furthermore, the significant antibiotic selection pressure from clinical and environmental sources is the cause of the rise in MDR. Staphylococcus species are the most frequent etiological bacteria responsible for diabetic foot ulcer infections (Goudarzi *et al*., 2016). Even though S. aureus is a naturally occurring or invasive bacterium that inhabits the skin, nose, and mucous membranes of the human respiratory system, it can cause a variety of diseases, including bacteremia, pneumonia, skin and soft tissue infections such as abscesses, boils, post-operative wound infections, Toxic Shock syndrome and Scalded Skin Syndrome (Asanin *et al*., 2019). Staphylococcus is found naturally in about 30% of healthy people, yet it is one of the most common pathogenic bacteria in the community and hospitals (Tong *et al*., 2015). Pyogenic Staphylococcus infections are frequently more dangerous because of their resistance to various antibiotic classes (Rao *et al*., 2014). Vancomycin was selected as the last line of treatment for Methicillin-Resistant Staphylococcus aureus (MRSA) infections since it is the most significant strain with multiple antibiotic resistance and has grown to be a significant issue for hospital infections (Reddy *et al*., 2014). However, as bacterial growth inhibition rates are higher when using nanoparticles and antibiotics together than when using them separately, nanoparticles and antibiotics demonstrated a synergistic impact against bacteria (Fayaz *et al*., 2010). Conversely, zinc oxide makes hydrogen peroxide (H_2O_2), which has fetal antibacterial properties (Yamamoto *et al*., 2004). By increasing the production of Reactive Oxygen Species (ROS) and inhibiting hemolysis caused by pathogen-produced hemolysin toxins, ZnO nanoparticles break down the bacterial cell membrane, decrease the hydrophobic surface of the cell, and reduce the production of the oxidative stress genes in bacteria (Pati *et al*., 2014). Vancomycin and Linezolid are the only recommended treatments for severe MRSA infections; Clindamycin and Macrolides are better choices for less serious infections. Due to the overuse of glycopeptide antibiotics prompted by the global spread of MRSA, MRSA isolates have become less susceptible to vancomycin, resulting in treatment failure (Ikeda-Dantsuji *et al*., 2011). It is hypothesized that a contemporaneous increase in the MIC values of other anti-MRSA medicines may be linked to the change in Vancomycin MIC (minimum inhibitory concentration) values (Ikeda-Dantsuji *et al*., 2011; Chang *et al*., 2014). By selectively inhibiting a more vulnerable subgroup of heterogenic S. aureus, fluoroquinolone exposure affects Oxacillin resistance and may ultimately result in treatment failure (Venezia *et al*., 2001).

The current study aimed to isolate and diagnose multiple antibiotic-resistant S. aureus (SA), especially ORSA, MRSA (Oxacillin or Methicillin Resistant SA), and VISA, VRSA

(Vancomycin-intermediate or Resistant SA) from different diabetic foot ulcers. In addition to studying the prevalence of resistance to treatments with the presence of nanoparticles among the resistant bacterial isolates and determining the minimum inhibitory concentration (MIC) of specific antibiotics, zinc oxide in nano-sizes, and the synergistic effect of selected antibiotics, as part of the protocol procedure of treatment with routine antibiotics.

MATERIALS AND METHODS.

1. Isolation of Diabetic Foot Ulcer Bacteria

Diabetic foot ulcers clinical samples (108) were collected from Hospitals and the Public Health Laboratory patients in Cairo, Egypt, from September 2021 to December 2022. Skin surface infection samples were obtained (16 samples), wounds (38 samples), and pus (54 samples) for both sexes. Mannitol salt agar (MSA, Oxoid) cultivated clinical samples. To identify staphylococcal species, several morphological and biochemical characteristics were used, such as the hemolysis, catalase, and coagulase enzyme tests, as well as sensitivity to 5 µg of Oxacillin-Cefoxitin-Vancomycin (OX-FOX-VA) and 30 µg Cefoxitin-Vancomycin-Linezolid (FOX-VA-LN) antibiotic disks. At the same time, the Kirby-Bauer disc diffusion method was used for sensitivity testing (Kirby-Bauer *et al*., 1966), according to Clinical Laboratory Standard Institute recommendations (CLSI, 2021).

2. Synthetases of ZnO-nanoparticles

A new sol-gel approach was performed to synthesize ZnO nanoparticles by mixing 8.14 g ZnSO4.7H2O (Merck) and 30 ml diethylene glycol, then 30 ml ethanol (99.7%) and 900 ml dH2O were added. The mixture was stirred for two hours at 85°C to form the gel using a magnetic stirrer. In an oven, the gel was dried at 220^{o}C for one hour and was ground to a final powder or particles as described by Jurablu *et al*. (2015).

3. ZnO-nanoparticles characterization

A Philips PAN analytical instrument was employed for X-ray diffraction studies. X-ray diffraction investigations with a bond angle of 3˚ and a scanning range of 20˚ to 80˚ determined the phase variety and particle size. A Perkin Elmer spectrophotometer characterized the ZnO nanoparticles, and the attached functional groups to the surface of the produced ZnO nanoparticles were studied and characterized using a Fourier transform infrared spectrometer (FT-IR spectrometer) with a scanning range of 4000-400 cm^{-1} and a resolution of 4 cm^{-1}. (Mendes *et al*., 2021). On the other hand, transmission electron microscopy (TEM) is a microscopy technique in which an electron beam is directed onto and passed through a fragile material. In TEM research, the image is focused on a 400-mesh imaging device (Hitachi H-7100 electron microscopy sciences) after being enlarged (Fahim & Hussein, 2017).

4. Determination of Minimum Inhibitory Concentration (MIC)

The modified macro-double dilution method was used, based on the method of Saginur *et al*., 2006. One milliliter of Mueller-Hinton broth was added to some test tubes. Then, one ml of pre-prepared concentrations of 20 microgram (µg) for each antibiotic or 20 millimole for ZnO-NPs calculating as ZnO molecular weight (MW: 81.38) at broth media, 1000 µl was added to tube No.1. The materials were mixed by using a micropipette by withdrawing the culture 10 times to obtain a concentration of 10 µg/ml for antibiotic and 10 mM for ZnO-NPs. Progressive dilutions were transferred from tube No.1 to other tubes, and the process was repeated up to tube No.15. Mix in the same previous way to obtain a concentration of 0.5 µg/ml for antibiotics or 0.5 nM for ZnO-NPs. Thus, the concentrations were 15 (0.5 to 10) µg/ml for the antibiotic and nM for ZnO-NPs. Compared to the third McFarland tube, 100 µl of bacterial suspension was added and cultured for 18 hours at a concentration of 1.5×10^5 cells/ml. As a positive control, only add the bacterial suspension and Mueller-Hinton broth to tube No.

16. The Mueller-Hinton broth is the only negative control in Tube No. 17. Tubes were incubated at 37°C for 18-24 hours. Examination of bacterial growth, the MIC, and the lowest inhibitory concentration of the antibiotic or ZnO-nanoparticles was observed (no visible growth).

5. Study the synergistic effect of antibiotics with nanoparticles

Based on the method of Saginur *et al*. (2006, the modified macro-double dilution method was used by adding 1000 µl Mueller-Hinton broth to 10 test tubes. To study the synergistic effect of the nanoparticles with the antibiotics, the first tube was filled with 1000 µl of medium containing the MIC concentration for each antibiotic and the ZnO nanoparticles established in the previous phase. A micropipette mixed the mixture many times, then 1000 µl from tube No.1 was transferred to tube No.2, which also contains 1000 µl of the nutrient broth, and mixed well. The process was repeated for tube No.10. An 18-hour-old bacterial culture was added (100 µl) at a concentration of 1.5 × 10^8 cells/ml compared to the third tube of McFarland tubes. Finally, tubes were incubated at 37ºC for 18-24 hours till the bacterial growth was visible, and the syn-MIC was observed to obtain the lowest inhibitory concentration of the antibiotic antagonist synergistic with ZnO nanoparticles.

Statistical analysis

Each experiment was carried out in triplicate, and the average values were recorded with their standard deviations. The probability value for the statistical test was 0.5%, which was used to compare the differences between the inhibition zones and minimal inhibitory concentrations.

RESULTS AND DISCUSSION

1. Isolation and identification of MDR *S. aureus* isolates.

The diabetic foot ulcers clinical samples were enumerated in MSA culture media, and the total positive growth was 87(108), indicated as Staphylococcus species. The Gram-positive Staphylococcus aureus golden morphological colonies and positive for hemolysis, catalase, and coagulase enzyme tests were classified as *S. aureus* species. At the same time, the coagulase-negative susceptible species to 5 µg of Oxacillin-Cefoxitin-Vancomycin (OX-FOX-VA) were identified as other Staphylococcus types (epidermis, saprophytic, or other types). The diabetic foot ulcers clinical samples were enumerated in MSA and/or ORSAB culture media, the positive samples, which were obtained from the skin surface infections, were 11(16), with the percentage of 68.75%, wounds were 23(38), with a percentage of 60.52%, and the pus was 53(54), with a percentage of 98.15%. While the total positive growth was 87(108), which was 80.56%, and all were investigated as *Staphylococcus* species. However, the Gram-positive staphylococci with yellow or golden morphological colonies on MSA media and positive for hemolysis, catalase, and coagulase enzyme tests were classified as *S. aureus* species. The (ORSA and MRSA) *S. aureus* species types were blue colonies on ORSAB media.

2. ZnO-nanoparticles characterization

2.1. X-ray diffraction analysis (XRD)

The ZnO crystallite was consistent with the XRD peaks. Because of the cleanliness of the material used in producing ZnO-NPs, the analysis revealed no additional peaks. The Joint Committee on Powder Diffraction Standards, 36-1451 database (JCPDS) revealed the same pattern in the diffraction peak positions. However, the diffraction peaks of ZnO-NPs correspond to the values (2θ) degrees. High diffraction peaks indicated the crystalline nature of the material, which shows the values of the structural parameters used to calculate the size of the ZnO-nanoparticles crystallite according to Vijayakumara *et al*. (2018). The XRD pattern of the as-prepared and annealed powder samples is shown in Figure 1. The XRD pattern of the as-prepared and annealed powder samples is shown in Figure 1. The as-prepared sample's XRD pattern demonstrates that ZnO's crystalline phase had not been induced. Conversely, the annealed powdered samples show a long-range order of

sharp Bragg peaks. Each peak's Miller index correlates with ZnO's typical hexagonal wurtzite structure. The ZnO-NPs annealed from 300 to 600°C displayed similar Bragg peak patterns. The XRD peaks appearing at 2θ of ~31°, ~34°, ~36°, ~47°, ~56°, ~62°, ~66°, ~67°, ~69° and ~73° corresponding to the (100), (002), (101), (102), (110), (103), (200), (112), (201) and (202) planes, respectively, which are in agreement with the Joint Committee on Powder Diffraction Standard, JCPDS (Card Number 36-1451). The complete breakdown of the precursor and the resulting pure production of ZnO-NPs are shown by the absence of diffraction peaks from other species, and the entire width at half maximum decreases with increasing annealing temperature. It is evident that as the annealing temperature is raised, the size and crystallinity of ZnO-NPs increase. The average crystallite sizes determined by the relation were around 29.2 nm at 300°C, 33.6 nm at 400°C, 35.5 nm at 500°C, and 41.6 nm at 600°C. This supports the finding by Salavati *et al.* (2008) that the average size of ZnO nanoparticles increases as the annealing temperature rises.

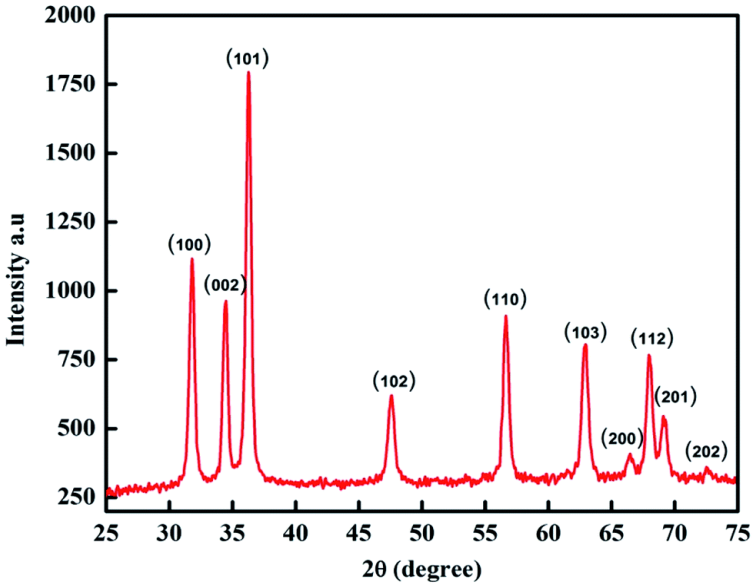

Fig. (1): XRD patterns of ZnO nanoparticles

2.2. Fourier transform infrared spectroscopy

On the other hand, the FTIR spectrum of all the ZnO samples produced through various methods proved that the final product formed is ZnO in both cases. Herein, one as-synthesized sample was also recoded, and the graph plotted above in black shows that an intermediate product is formed, eventually leading to pure ZnO after calcination. IR analysis records the bending vibrations of various bonds like C-O, C-H, O-H, etc., indicating the presence of different functional groups in the sample. Figure 2 shows a series of absorption peaks in the 400 to 4000 cm-1 range. According to Xing *et al.* (2011), the O-H stretching vibration of the intramolecular hydrogen bond is represented by the faint peaks at 3713 cm^{-1} and 2346 cm^{-1}. The intensity of the peaks assigned to the O-H bond decreased with increasing temperature. This might be due to the removal of some organic material. The doublet peaks seen at 1690 are associated with the C=O symmetric stretching vibration of zinc carboxylate. The bending vibration of C-H stretching is responsible for the absorption peaks at about 1533 cm^{-1}. The peak is significantly reduced by annealing at 600°C, suggesting that the organic material has been eliminated at this

temperature. It is evident that at this temperature, this particular peak is not abolished. The stretching of the C-O bond is responsible for the peak centered at 1210 cm^{-1}. This peak deteriorates with increasing temperature and nearly disappears at the 600°C annealing temperature. The Zn-O stretching mode is responsible for the strong peak at about 575 cm^{-1}. The spectrum of other two final samples was observed which was similar to the previously reported ZnO FTIR spectra according to Wang *et al*. (2017).

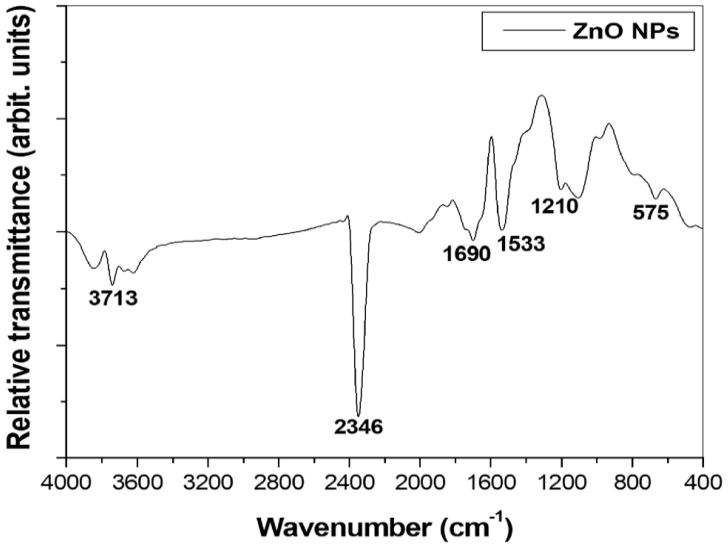

Figure (2). The FTIR pattern of the ZnO nanoparticles

2.3. Transmission Electron Microscopy

One of the most crucial microscopic techniques in nanotechnology for describing materials at length scales ranging from atoms to hundreds of nanometers is transmission electron microscopy (TEM). This method involves passing an electron beam through an ultrathin object (often less than 100 nm) and interacting with it. At resolutions of 0.1 nm, modern TEMs can directly view atoms in crystalline materials. To examine the quality, shape, size, and crystal structure features, including grain boundaries and dislocations, high-resolution TEM (HRTEM) is utilized, as illustrated in Figure 3, which displays a TEM image of the ZnO-NPs. The size of the ZnO-NPs seen under TEM was consistent. Agglomeration was frequent because of ZnO-NPs' minimal size and high surface energy. The image indicates that the powder is made up of quasi-spherical nanoparticles, and it was noted that the morphology of the ZnO-NPs had expanded into a nearly hexagonal shape. The majority of ZnO-NPs that were measured had an average size of 40 nm and a diameter between 30 and 50 nm. This closely matches the findings from the powder's XRD tests. The XRD calculation assesses the extended crystalline region that coherently diffracts X-rays, whereas TEM results are based on the visible grain boundaries (Bandyopadhyay *et al.*, 2002). Although the quantity of nanoparticles and the type of organic solvent may vary depending on the particular target matter, TEM is effective and somewhat precise in assessing the size of nanoparticles and may eventually become a standard process. More changes to the approach are required to increase accuracy and speed up the process. Additionally, because smaller nanoparticles gathered and formed larger particles, nearly all of the ZnO nanoparticles emerged in clusters of nanorods (Sabita *et al.*, 2017).

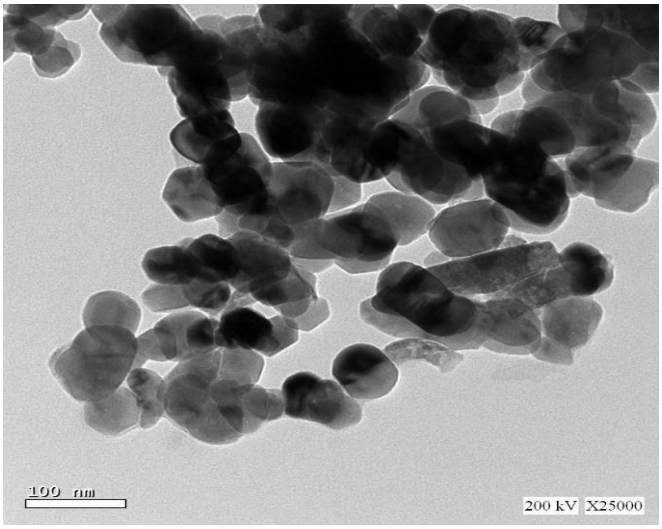

Figure (3): TEM images of ZnO nanoparticles

3. Determination of MIC and syn-MIC for MDR *S. aureus* isolates.

The diabetic foot ulcers clinical samples were enumerated in MSA culture media, and the positive growth of 87(108) was indicated as Staphylococcus species. The Gram-positive Staphylococcus aureus golden morphological colonies and positive for hemolysis, catalase, and coagulase enzyme tests were classified as *S. aureus* species. In contrast, the coagulase-negative susceptible species to 5 µg of Oxacillin-Cefoxitin-Vancomycin (OX-FOX-VA) were identified as other staphylococcus types (epidermis, saprophytic, or other types). All staphylococcus isolates 87 (80.56%), which were isolated from infected skin surface, 11(16), 53(54) pus cells, and 23(38) wounds for both sexes, undoubtedly belonged to S. aureus as shown in Table 1. The infection by the MDR strain of S. aureus was represented at 21.3 % among all other causes of staphylococcal diabetic foot ulcers. However, 14.81, 4.63, and 1.85 % represent heterogenous hORSA, MRSA, and VISA *S. aureus*. No evidence indicates detecting each VRSA or LRSA *S. aureus* phenotype. Similar observations were reported by Steinkraus *et al.* (2007) and Panda *et al.* (2016).

Table 1: Identification and selection of *Staphylococcus aureus* DFU isolated bacteria.

Infected skin sample type	Growth in MSA media		Bacterial Antibiotics Susceptibly†							
	Number of growths (Total)	Percentage %	Oxacillin† ORSA Types		Cefoxitin† MRSA Types		Vancomycin† VISA Types		Vancomycin-Linezolid† VRSA or LRSA Types	
			R*	Percent %	R*	Percent %	R*	Percent %	R*	Percent %
Wounds	23 (38)	60.52 %	5 (23)	21.74%	0 (23)	0.00 %	0 (23)	0.00 %	0 (23)	0.00 %
Puss cells	53 (54)	98.15 %	11 (53)	20.75%	5 (53)	9.43 %	2 (53)	3.77 %	0 (53)	0.00 %
Skin surface	11 (16)	68.75 %	0 (11)	0.00%	0 (11)	0.00 %	0 (11)	0.00 %	0 (11)	0.00 %
TOTAL	87 (108)	80.56 %	16 (87)	18.39%	5 (87)	5.74 %	2 (87)	2.29 %	0 (87)	0.00 %
Strain type	23 (108) MDR *Staphylococcus aures*		16 (108) ORSA strains		5 (108) MRSA strains		2 (108) VISA strains		(ND) VRSA or LRSA strains	
Percentage%	21.30 %		14.81 %		4.63 %		1.85 %		0.0 %	

R*: Antibiotic-resistant Staphylococcus aureus strains.

†Oxacillin (OX) resistant strains less than 17 mm - sensitive more than 18 mm.

†Cefoxitin (FOX) resistant *S. aures* strains less than 21 mm - sensitive more than 22 mm.

†Cefoxitin (FOX) resistant *S. epidermidis* strains less than 24 mm - sensitive more than 25 mm.

†Vancomycin (VA) or Linezolid (LN) - (30) µg resistant strains less than 21 mm - sensitive more than 22.

On other side, the (23) isolates (16) $_{H}$ORSA, (5) MRSA and (2) VISA given laboratory code name by (SMG $_{HORSA}$ from 01 to 16), (SMG $_{MRSA}$ from 17 to 21) and (SMG $_{VISA}$ 22 and 23), respectively as shown in (Table 2). From the presented data, the treatment by ZnO-NPs inhibited the growth of ORSA, MRSA, and VISA phenotypes by the individual minimal inhibitory concentration MIC with an average of 5.21 mM/ml. At the same time, they give MIC average values of 3.49, 2.6, 2.99, and 1.99 µg/ml for (OX, FOX, VA, and LN) individual antibiotics, respectively, with similar observations by Panda et al. (2016). In the same aspect, the use of MIC µg/ml values of antibiotics supported with MIC of ZnO-NPs mM/ml by (1:1) led to a decrease in syn-MICs inhibition values by 1.13, 0.59, 1.0 and 0.63 for each antibiotic supported with ZnO-NPs by mM/ml with synergistic effect percentage of 309, 441, 299 and 316 %, respectively as shown in Table (2).

Table 2: Determination of MIC and syn-MIC for MDR *Staphylococcus aureus* isolated strains.

Staphylococcus aureus **Laboratory code name**	**Strain type**		**Individual Minimal Inhibitory Concentrations**					**Synergistic Minimal Inhibitory Concentrations**			
			ZnO-NPs (mM/ml)	**Individual MIC Antibiotics (µg/ml)**				**syn-MIC Antibiotic + ZnO-NPs (µg + mM/ml*) (1:1)**			
			NPs	**OX**	**FOX**	**VA**	**LN**	**OX+NPs**	**FOX+NPs**	**VA+NPs**	**LN+NPs**
SMG $_{ORSA}$ 01:16	hMDR†	ORSA	5.19 ±0.24	7.44 ±0.71	0.75 ±0.31	2.53± 0.28	2.65 ±0.22	0.78±0.25	0.56 ±0.17	0.56±0.17	0.53±0.12
SMG $_{MRSA}$ 17:21	mMDR††	MRSA	5.20 ±0.27	1.30 ±0.27	5.03 ±0.45	0.07 ±0.27	0.60 ±0.22	0.60±0.22	0.70 ±0.27	0.70±0.27	0.60±0.22
SMG $_{VISA}$ 22:23	mMDR††	VISA	5.25 ±0.35	1.75 ±0.35	1.75 ±0.35	5.75 ±0.35	2.75 ±0.35	2.00±0.00	0.50 ±0.00	1.75±0.35	0.75±0.35
Individual MIC Average			5.21 ±0.06	3.49 ±0.23	2.60 ±0.07	2.99 ±0.05	1.99 ±0.08	1.13±0.14	0.59 ±0.14	1.00±0.09	0.63±0.12
6 Percentage of antibiotics ZnO-NPs synergetic effect								309 %	441 %	299 %	316 %

* µg/ml = mM/ml x (MW) molecular wight.

† mMDR: Monogenous Multidrug Resistant.

†† hMDR: Heterogeneous Multidrug Resistant.

Methicillin resistance in S. aureus is caused by the mecA gene, which codes for a modified penicillin-binding protein with a lower affinity for β-lactam antibiotics, making it resistant to all of them. All five MRSA isolates in the current investigation were detected using cefoxitin. However, five were not identified using the Oxacillin screen test since their Oxacillin MIC was less than 2 µg/ml. Other researchers also made similar findings (Sahai *et al*., 2014; Panda *et al*., 2016). The fact that cefoxitin is a more effective inducer of the mecA gene than oxacillin may help to explain these observations (Sharma *et al*., 2017). In the same aspect, Vancomycin has been recommended for serious MRSA infections, whereas Linezolid and Daptomycin have been recommended for skin and soft tissue infections. Recent studies have reported reduced efficacy of Vancomycin against MRSA infections, and subtle changes in the MIC may lead to clinical failure. Therefore, alternative anti-MRSA medicines need to be taken into account for therapy. Because of its intense antibacterial action against gram-positive bacteria and good short-term safety record, linezolid has also been used to treat severe infections. Compared to vancomycin resistance, fewer reports of Linezolid resistance among S. aureus phenotypes exist; nonetheless, the available data is restricted (Chang *et al*., 2015; Shariq & Tanvir, 2017). Since all resistant S. aureus isolates were consistently responsive to

Linezolid in most literature, the clinical incidence of Linezolid resistance is uncommon. It has only been reported to occur after extended therapy for no more than two weeks, as Iguchi *et al.* (2016) reported.

Conclusion

The effectiveness of ZnO-NPs as an antibacterial agent in treating MDR S. aureus infections is supported by current data. Even though we did not observe any Vancomycin or Linezolid resistance in the MDR isolates, we should keep a close eye on antibiotic selection pressure and creeping MIC to help detect resistance early. This study also emphasizes the limited usage of antibiotics inappropriate for Methicillin-Susceptible or Vancomycin-Linezolid for isolates of ORSA, MRSA, and VISA S. aureus. Alternative treatment approaches should also be investigated, such as the synergism with nanoparticles, particularly ZnO-NPs, for less severe MDR infections, while keeping Vancomycin and Linezolid for life-threatening infections. Identifying the emergence of resistant isolates early may be easier if MIC shifts are continuously monitored, even in the susceptible range. Given the constant risk of resistance developing through a novel mechanism, this study emphasizes the necessity to control rather than treat ORSA, MRSA, and VISA infections.

Recommendations

Based on the encouraging results achieved here, this study suggests using ZnO-NPs as an adjuvant with other antibiotics that target MDR S. aureus in order to limit infection with this pathogen. We propose that ZnO-NPs are promising nano metal oxides that may be useful for the biomedical therapy of diabetic foot ulcers by lowering the resistance-related phenotypes, since this finding suggests a synergistic effect of the combination of ZnO-NPs and tested antibiotics.

Conflicts of Interest

The authors declare no conflict of interest.

REFERENCES

Abdel Rahman, A.T.; Hafez, S.F. and Abdelhakam, S.M. (2010). Antimicrobial resistant bacteria among health care workers in intensive care units at Ain Shams University Hospitals. J Egypt Soc Parasitol, 40(1): 71-84.

Asanin, J.; Misic, D.; Aksentijevic, K.; Tambur, Z.; Rakonjac, B.; Kovacevic, I.; Spergser, J. and Loncaric, I. (2019). Genetic Profiling and Comparison of Human and Animal Methicillin-Resistant Staphylococcus aureus (MRSA) Isolates from Serbia. *Antibiotics*, 8(26): 1-12. doi:10.3390/antibiotics8010026.

Bandyopadhyay, S.; Paul, G.K.; Roy, R.R. and Sen, S.K. (2002). Study of structural and electrical properties of grain-boundary modified ZnO films prepared by sol-gel technique. Chem Phys, 74: 83-91.

Chang, W.; Ma, X.; Gao, P.; Lv, X.; Lu, H. and Chen, F. (2015). Vancomycin MIC creep in methicillin-resistant *Staphylococcus aureus* (MRSA) isolates from 2006 to 2010 in a hospital in China. Indian J Med Microbiol., 33(2): 262- 266.

Clinical and Laboratory Standards Institute, CLSI (2021). Performance Standards for Antimicrobial Susceptibility Testing. 31st ed. CLSI supplement M100.; 39(1): 42-67.

Fahim, S. and Hussein, W. (2017). Antibacterial Potentials of Surfactins against Multidrug Resistant Bacteria. Research Journal of pharmaceutical biological and chemical sciences; 8(3): 1076-1083.

Fayaz, A.M.; Balaji, K.; Girilal, M.; Yadav, R.; Kalaichelvan, P.T. and Venketesan, R. (2010) Biogenic synthesis of silver nanoparticles and their synergistic effect with antibiotics: a study against gram-positive and gram-negative bacteria. Nanomedicine; 6(1): 103-9. https:// doi: 10.1016/j.nano.2009.04.006.

Gordon, T.; Perlstein, B. and Houbara, O. (2011). Synthesis and characterization of zinc/iron oxide composite nanoparticles and their antibacterial properties. Colloids Surf A.; 374(1): 1-8.

Goudarzi, G.; Tahmasbi, F.; Anbari, K. and Ghafarzadeh, M. (2016). Distribution of genes encoding resistance to macrolides among staphylococci isolated from the nasal cavity of hospital employees in Khorramabad, Iran. Iranian Red Crescent Medical Journal; 18: 25701-25711.

Iguchi, S.; Mizutani, T.; Hiramatsu, K. and Kikuchi, K. (2016). Rapid acquisition of linezolid resistance in methicillin-resistant *Staphylococcus aureus*: Role of hyper-mutation and homologous recombination. *PLoS One*.; 11(5):1-13.

Ikeda-Dantsuji, Y.; Hanaki, H.; Nakae, T.; Takesue, Y.; Tomono, K. and Honda, J. (2011). Emergence of Linezolid-Resistant Mutants in a Susceptible-Cell Population of Methicillin-Resistant *Staphylococcus aureus*. *Antimicrob Agents Chemother*.; 55(5): 2466-2478.

Jacob, S.P.; Bharathkumar, R. and Ashwathram, G. (2014). *Aspergillus niger* mediated synthesis of ZnO nanoparticles and their antimicrobial and in vitro anti-cancerous activity. World J Pharm Res.; 3(2): 3044-3054.

Jurablu, S.; Farahmandjou, M. and Firoozabadi, T.P. (2015). Sol-Gel Synthesis of Zinc Oxide (ZnO) Nanoparticles, Study of Structural and Optical Properties. Journal of Sciences, Islamic Republic of Iran; 26(3): 281-285.

Kabata-Pendias, A. and Mukherjee, A.B. (2007). Trace Elements from Soil to Human. Berlin, Heidelberg: Springer.

Kirby-Bauer, A.W.; Sherris, J.C. and Turck, M. (1966). Antibiotic susceptibility testing by standardized single disc method. American Journal of Clinical Pathology; 45(4): 493-496.

Mendes, C.R.; Dilarri, G.; Stradioto, M.R.; Lopes, P.R.M.; Bidoia, E.D. and Montagnolli, R.N. (2021). Zeta potential mechanisms applied to cellular immobilization: A study with *Saccharomyces cerevisiae* on dye adsorption. J. Polym. Environ.; 29: 2214-2226.

Panda, R.K.; Mahapatra, A.; Mallick, B. and Chayani, N. (2016). Evaluation of Genotypic and Phenotypic Methods for Detection of Methicillin Resistant *Staphylococcus aureus* in a Tertiary Care Hospital of Eastern Odisha. J Clin Diagn Res.; 10(2):19-21.

Pati, R.; Mehta, R.K.; Mohanty, S.; Padhi, A.; Sengupta, M.; Vaseeharan, B.; Goswami, C. and Sonawane, A. (2014). Topical application of zinc oxide nanoparticles reduces bacterial skin infection in mice and exhibits antibacterial activity by inducing oxidative stress response and cell membrane disintegration in macrophages. Nano-medicine; 10(6): 1195-1208.

Rao, K.A.; Deepa, S. and Venkatsha, D. (2014). Screening for nasal colonizer: Mandatory to prevent surgical site infections. International Journal of Scientific Study; 2(5): 1-5.

Reddy, P.N.; Srirama, K. and Dirisala, V.R. (2017). An Update on Clinical Burden, Diagnostic Tools, and Therapeutic Options of *Staphylococcus aureus*. *Infectious Diseases: Research and Treatment*; 10: 1-15.

Sabita, S.; Subash, C.B.; Shankar, P.S. and Leela, P.J. (2017). Synthesis and study of zinc oxide nanoparticles for dye sensitized solar cell. Research Journal of Physical Sciences; 5: 6-10.

Saginur, R.; Denis, M.S.; Ferris, W.; Aron, S.D.; Chan, F.; Lee, C. and Ramotar, K. (2006). Multiple Combination bactericidal testing of Staphylococcal biofilms from implant-associated infections. Antimicrobial Agents and Chemotherapy; 50(1): 55-61.

Sahai, S.; Prasad, S. and Chauhan, M. (2014). Comparative Evaluation of Oxacillin and Cefoxitin disk Diffusion Method in Detection of Methicillin- resistant *Staphylococcus aureus* (MRSA) Isolates from a Tertiary Care Hospital in North India. Int J SciStudy.; 2(6): 125-138.

Salavati-Niasari, M.; Davar, F. and Mazaheri, M. (2008). Preparation of ZnO nanoparticles from [bis(acetylacetonato)zinc(II)]- oleyl amine complex by thermal decomposition. *Mater. Lett.;* 62: 1890-1898.

Saxena, N.; Dadhich, D. and Maheshwari, D. (2013). Aerobic bacterial isolates from burn

wound infection patients and their antimicrobial susceptibility pattern in Kota, Rajasthan. J Evol Med Dent Sci.; 23(2): 4156-4160.

Şeker, S.; Elçin, A.E.; Yumak T, Sinag, A. and Elçin, Y.M. (2014). In vitro cytotoxicity of hydrothermally synthesized ZnO nano-particles on human periodontal ligament fibroblast and mouse dermal fibroblast cells. *Toxicol In Vitro.;* 28(8): 1349-1358.

Shariq, A. and Tanvir, S.B. (2017). Susceptibility profile of methicillin resistant *Staphylo coccus aureus* to linezolid in clinical isolates. Int J Health Sci (Qassim).; 11(1):1-4.

Sharma S, Srivastava P, Kulshrestha A, Abbas A (2017) Evaluation of different phenotypic methods for the detection of methicillin resistant *Staphylococcus aureus* and antimicrobial susceptibility pattern of MRSA. Int J Community Med Public Health.; 4(9): 3297-3301.

Steinkraus, G.; White, R.; Friedrich, L. (2007). Vancomycin MIC creep in non-vancomycin-intermediate *Staphylococcus aureus* (VISA), vancomycin-susceptible clinical methicillin-resistant S. aureus (MRSA) blood isolates from 2001-2005. J Antimicrob Chemother.; 60(4): 788-794.

Tong, S.Y.; Davis, J.S.; Eichenberger, E.; Holland, T.L. and Fowler, V.G. (2015). *Staphylococcus aureus* infections: Epidemiology, path physiology, clinical manifestations and management. Clinical Microbiology Reviews; 28(3): 603-661.

Venezia, R.A.; Domaracki, B.E.; Evans, A.M.; Preston, K.E. and Graffunder, E.M. (2001). Selection of high-level oxacillin resistance in hetero-resistant *Staphylococcus aureus* by fluoroquinolone exposure. J Antimicrob Chemother.; 48(3): 375-381.

Verma, R.; Naik, K.K.; Gangwar J. and Srivastava, A.K. (2014). Morphology, mechanism and optical properties of nanometer sized MgO synthesized via facile wet chemical method. Mate Chem Phys.; 148(3):1064-1070.

Vijayakumara, S.; Mahadevana, P.; Arulmozhia, S. and Sriramb, P.K. (2018). Green synthesis of zinc oxide nanoparticles using *Atalantia monophylla* leaf extracts: Characterization and antimicrobial analysis. Mater. Sci. Semicond. Process.; 82: 39-45. https:// doi.org/10.1016/j.mssp. 2018. 03.017.

Wang, J.; Lee, J.S.; Kim, D. and Zhu, L. (2017). Exploration of zinc oxide nanoparticles as a multitarget and multifunctional anticancer nanomedicine. ACS applied materials & interfaces; 9(46): 39971-84.

Wang, L.; Hu, C. and Shao, L. (2017). The antimicrobial activity of nanoparticles: present situation and prospects for the future. Int J Nanomedicine.; 12: 1227-1249.

Xing, Z.; Geng, B.; Li, X.; Jiang, H.; Feng, C. and Ge, T. (2011). Self-assembly fabrication of 3D porous quasi-flower-like ZnO nanostrip clusters for photodegradation of an organic dye with high performance. *CrystEngComm.;* 13: 2137-214.

Yamamoto, O.; Komatsu, M.; Sawai, J. and Nakagawa, Z.E. (2004). Effect of lattice constant of zinc oxide on antibacterial characteristics. Journal of Materials Science: Materials in Medicine; 15: 847-851.

Zhao, J.; Fan, B.; Wu, Z.; Xu, M. and Luo, Y. (2015). Serum zinc is associated with plasma leptin and Cu-Zn SOD in elite male basketball athletes. J Trace Elem Med Bio.; 30:49-53.

تأثير جزيئات أكسيد الزنك النانوميترية على مقاومة المضادات الحيوية لبكتريا الأستافيلوكوكس العنقودية المتلازمة لقرح القدم السكري

أمين حسين أمين[١] ، عادل السيد البلتاجى[٢]، صلاح منصور عبدالجواد[٣] ، سامح فهيم فرج الله[٢]

[١] المستشفى السعودي الألماني - قسم المعامل وبنك الدم - القاهرة - مصر .

[٢] الميكروبيولوجيا الزراعية بقسم النبات - كلية الزراعة - جامعة المنوفية.

[3] قسم الكيمياء الحيوية الزراعية - كلية الزراعة - جامعة المنوفية - مصر.

الملخص العربي

في العقود الماضية، كان المعدل المتزايد لمقاومة المضادات الحيوية عائقًا حاسمًا أمام نجاح علاج العديد من الأمراض البكتيرية. هناك أيضًا طلب كبير على ابتكار مواد نانومتريه جديدة تساهم في تطوير المركبات الحيوية المضادة للميكروبات والتي حتماً فتحت آفاقًا علاجية جديدة في الأساليب الطبية الرائجة. ومن خلال بذل العديد من الجهود لتخليق جسيمات نانومتريه جديدة من أكسيد المعادن تكون قادرة علي التحكم بشكل أفضل في جرعات العلاج المستخدمة للحد من البكتريا متعددة المقاومة الملازمة لقرح القدم السكري. حيث في الآونة الأخيرة، تعتبر أكاسيد المعادن عوامل غير عضوية عالية الكفاءة ذات خصائص مضادة للميكروبات. ففي هذه الدراسة، تم تخليق أكسيد الزنك النانوميتري باستخدام طريقة السول جل. والتي تم تعريضها للفحص بالأشعة السينية والأشعة تحت الحمراء وكذلك التصوير بالمجهر الإلكتروني الماسح. حيث كشفت التقنيات المستخدمة للتوصيف عن تخليق طور نقي من أكسيد الزنك النانوميتري غير المتكتل ذات أحجام تتراوح أقطارها بين ٣٠ الى ٥٠ نانومتر بمتوسط حجم قطر ٤٠ نانومتر. كما أظهرت صور المجهر الإلكتروني الماسح أشكال سداسية متعددة الأوجه. على صعيد أخر تمثل الإصابة ببكتيريا الأستافيلوكوكس أورس متعددة المقاومة ٢١,٣ % بين مسببات قرح القدم السكرية العنقودية. حيث أدت معاملة تلك السلالات بواسطة أكسيد الزنك النانوميتري إلى تثبيط نمو أنواع الأستافيلوكوكس أورس المقاومة للأوكسيسلين غير المتجانسة والأنواع المقاومة للميثسيلين والمتوسطة المقاومة للفانكومايسين بمتوسط أقل قيم تركيزات مثبطة بلغت ٥,٢١ مللي مول لكل ملليتر. في حين أنها أعطت متوسطات قيم أقل تركيز مثبط ٣,٤، ٢,٩٩، ٢,٦و ١,٩٩ ميكروجرام لكل ملليتر على حدي من المضادات الحيوية (أوكسيسيلين، سيفوكستين، فانكوميسين ولينوزوليد) على التوالي. وفي نفس الجانب أدى استخدام أقل تركيزات مثبطة لكل من المضادات الحيوية المدعمة بأكاسيد الزنك النانوميترية بنسب (١:١) إلى انخفاض متوسطات قيم التثبيط بلغت نسبتها ٣٠٩، ٤٤١، ٢٩٩ و٣١٦ %، على التوالي. ويشير هذا الاكتشاف إلى وجود تأثير تآزري للجمع بين أكاسيد الزنك النانوميترية والمضادات الحيوية المستخدمة في العلاج، لذلك نقترح بأن أكاسيد الزنك النانوميترية مركبات نانوية واعدة يمكن تقييمها وتقديمها للعلاج البيولوجي الطبي لقرح القدم السكري وذلك عن طريق تقليل مقاومة تلك الأنواع الميكروبية للمضادات الحيوية والتي تلازم هذه القرح.

الكلمات المفتاحية: جزيئات ZnO النانوية؛ البكتيريا المقاومة للمضادات الحيوية؛ قرح القدم السكرية.